

Comparison of *NPN* transistors fabricated with broad beam and spatial profiling using focused beam ion implantation

S. D. Chu, J. C. Corelli, and A. J. Steckl

Center for Integrated Electronics, Rensselaer Polytechnic Institute, Troy, New York 12180

R. H. Reuss

Motorola Semiconductor Research and Development Laboratories, Phoenix, Arizona 85064

W. M. Clark, Jr. and D. B. Rensch

Hughes Research Laboratories, Malibu, California 90265

W. G. Morris

General Electric Corporate Research and Development Center, Schenectady, New York 12345

(Received 11 June 1985; accepted 26 September 1985)

The base region of *NPN* transistors was fabricated using a 0.2 μm beam diameter (maskless) of 75 keV B focused ion beam (FIB), and on the same wafer a broad beam (with mask) of 75 keV B ions with conventional ion implantation. Transistor properties were compared using electrical characteristics, microbeam Rutherford backscattering spectroscopy (RBS), and scanning Auger microscopy (SAM). No significant differences were found between the transistors fabricated with FIB and with conventional ion implantation. Lateral doping profiles were implanted using the FIB system. Bipolar transistors with lateral active base profiles implanted with FIB were shown to have normal device characteristics. While the main intent was to assess the feasibility of fabricating the devices, the expected relationships between lateral profile and base resistance and current gain were observed. The results indicate that FIB can be used to study the impact of lateral profiles on device performance.

I. INTRODUCTION

Focused ion beam (FIB) technology recently has been developed to a point so as to make possible novel device fabrication processes due to its potential for direct maskless implantation on a resistless substrate. In recent years submicron diam beams of B, Si, and Be have been used to selectively implant submicrometer lines of dopant atoms in GaAs¹⁻³ to produce FET devices. In addition, fabrication of Si MOSFET devices using submicrometer beams of B and Si ions has been demonstrated.⁴

Additional applications of FIB can be found in recent papers dealing with high resolution lithography,^{3,5} enhanced etching of substrates,⁶⁻⁸ and fabrication resistors.⁷ The above represent but a small fraction of papers published recently on the subject of focused ion beam technology for VLSI applications.

In this paper we report the fabrication, microstructural properties, and electrical characteristics of FIB implanted bipolar *NPN* transistors and compare them to similar transistors fabricated using conventional broad beam ion implantation.

II. EXPERIMENTAL METHODS

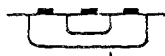
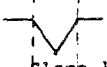
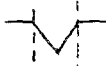
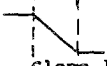
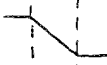


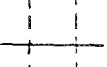
The *NPN* bipolar transistors were fabricated using both $\langle 100 \rangle$ and $\langle 111 \rangle$ oriented silicon wafers Sb doped to $\leq 0.02 \Omega \text{ cm}$ with 2.0 μm *n*-epi doped with As to 0.5 $\Omega \text{ cm}$. Details of the alignment for focused ion beam implantation of boron are given elsewhere.^{9,10} Only a portion of each wafer was given a FIB boron implant using a liquid metal ion source consisting of a boron-platinum eutectic (28% B, 78% Pt) on a rhenium tip. The FIB system is described elsewhere.¹¹ The energy of boron ion used in the FIB and conventional

broad beam implantation was 75 keV. The electrical contacts were deposited and patterned on TiW/Au metal. Insulation layers were Si₃N₄ and SiO₂ etched prior to Ohmic contact and metallization steps. The FIB system was used to fabricate different boron dopant profiles under the emitter region with three different base line dopings as given in Table I. The details of the process steps used to fabricate the *NPN* bipolar transistors were given in the earlier paper⁹ and will not be repeated here. The cross section of the test structure of *NPN* bipolar transistor is shown in Fig. 1.

In order to study what microstructural differences might exist between FIB and conventional implanted devices, we performed experiments using the Rutherford backscattering (RBS) method. These experiments were performed using a 2 MeV microfocused (2 μm diam beam spot on the sample) He⁺ beam. The He⁺ beam is first collimated down to a 10 μm beam aperture and then demagnified 10 \times using a combination of doublet quadrupole lenses, each consisting of one quadrupole electrostatic lens to focus the beam down to $\leq 2 \mu\text{m}$ diam. Using electrostatic scanning of the He⁺ beam a secondary electron image is formed of the surface under study. Although it is not possible to make a direct observation of the boron in the implanted region we were able to examine layers above and below the B implanted regions. This nondestructive method of analysis was used to look for microstructural differences such as disorder, impurities, and extent of different doped regions that might be found in FIB and conventional devices. Additional details giving a complete description of the method are published elsewhere.¹²

One additional surface analysis method was used to examine the structures for impurities (e.g., Pt from liquid metal source) namely, scanning Auger microscopy (SAM). The

TABLE I. Electrical parameters of different base doping profile.

| | A (baseline=4x10 ¹² /cm ²) | B (baseline=8x10 ¹² /cm ²) | C (baseline=1.6x10 ¹³ /cm ²) | |
|---------------------|---|---|---|---|
| Average dose | 2.2x10 ¹³ ^A /4x10 ¹³ ^B /3.6x10 ¹³ ^C | 4.4x10 ¹³ ^A /8x10 ¹³ ^B /7.2x10 ¹³ ^C | 8.8x10 ¹³ ^A /16x10 ¹³ ^B /14.4x10 ¹³ ^C |  |
| β | 22 | 11 | 5 | |
| r_B (K Ω) | 0.655 | 0.51 | 0.37 |  |
| BV_{CEO} | 12.6 | 12.8 | 13.0 | Slope 10 |
| BV_{CBO} | 27.0 | 25.0 | 25.0 | (Type 1) |
| Average dose | 1.2x10 ¹³ /2x10 ¹³ /1.82x10 ¹³ | 2.4x10 ¹³ /4x10 ¹³ /3.64x10 ¹³ | 4.8x10 ¹³ /8x10 ¹³ /7.28x10 ¹³ | |
| β | 49 | 20 | 7.5 | |
| r_B (K Ω) | 0.74 | 0.575 | 0.43 |  |
| BV_{CEO} | 11.9 | 12.1 | 13.5 | Slope 5 |
| BV_{CBO} | 27.5 | 27.2 | 22.5 | (Type 2) |
| Average dose | 2.2x10 ¹³ /2.2x10 ¹³ /2.2x10 ¹³ [*] | 4.4x10 ¹³ /4.4x10 ¹³ /4.4x10 ¹³ | 8.8x10 ¹³ /8.8x10 ¹³ /8.8x10 ¹³ | |
| β | 28 | 11 | 6 | |
| r_B (K Ω) | 0.79 | 0.58 | 0.45 |  |
| BV_{CEO} | 12.6 | 12.5 | 13.0 | Slope 10 |
| BV_{CBO} | 27.0 | 25.0 | 23.0 | (Type 3) |
| Average dose | 1.2x10 ¹³ /1.2x10 ¹³ /1.2x10 ¹³ | 2.4x10 ¹³ /2.4x10 ¹³ /2.4x10 ¹³ | 4.8x10 ¹³ /4.8x10 ¹³ /4.8x10 ¹³ | |
| β | 55 | 23 | 9 | |
| r_B (K Ω) | 0.93 | 0.71 | 0.50 |  |
| BV_{CEO} | 11.0 | 12.0 | 12.8 | Slope 5 |
| BV_{CBO} | 28.5 | 28.0 | 24.0 | (Type 4) |
| Average dose | 2.2x10 ¹³ /4.0x10 ¹² /8x10 ¹² | 4.4x10 ¹³ /8x10 ¹² /1.6x10 ¹³ | 8.8x10 ¹³ /1.6x10 ¹³ /3.2x10 ¹³ | |
| β | 25 | 9 | 5 | |
| r_B (K Ω) | 0.86 | 0.68 | 0.50 |  |
| BV_{CEO} | 13.0 | 13.5 | 14.0 | Slope 10 |
| BV_{CBO} | 26.5 | 25.0 | 24.5 | (Type 5) |
| Average dose | 1.2x10 ¹³ /4.0x10 ¹² /5.8x10 ¹² | 2.4x10 ¹³ /8x10 ¹² /1.16x10 ¹³ | 4.8x10 ¹³ /1.6x10 ¹³ /2.32x10 ¹³ | |
| β | 55 | 19 | 7 | |
| r_B (K Ω) | 1.05 | 0.76 | 0.53 |  |
| BV_{CEO} | 12.0 | 13.0 | 14.0 | Slope 5 |
| BV_{CBO} | 28.0 | 27.5 | 24.5 | (Type 6) |
| Average dose | 4x10 ¹² | 8x10 ¹² | 1.6x10 ¹³ | |
| β | 110 | 68 | 28 | |
| r_B (K Ω) | 1.09 | 0.91 | 0.80 |  |
| BV_{CEO} | 11.0 | 11.5 | 12.0 | |
| BV_{CBO} | 32.0 | 28.0 | 27.0 | |

A Average base doping under the emitter (20x40 μm^2)

B Average base doping outside the emitter

C Average base doping across entire base (80x90 μm^2)

SAM system used a 3 keV electron beam of diameter $\sim 1 \mu\text{m}$ at the surface to be examined. A 5 keV argon beam was used to sputter the surface under examination step by step, to check the chemical constituents or impurities of the device active region.

The I - V characteristics and voltage breakdown were measured using a Tektronix 576 curve tracer. The common-emitter current gain was taken at a base current of 100 μA , while the value obtained for base resistance depends strongly on the measurement technique. We used the low-frequency pulse measurement method¹³ since we suppose the transistor is to be used in a switching application and the pulse measurement technique provides the most appropriate value.

III. RESULTS AND DISCUSSION

A. Microstructural analysis by RBS and SAM

A schematic of the NPN transistor fabricated for our studies is given in Fig. 1. The RBS measurements were made with a 2 μm diam beam incident from the top through the base contacts. In Fig. 2 we show the RBS spectra for the base regions of a conventional and a FIB device. The gold contact films were removed from the contact windows before RBS measurements. The only observable difference in the spectrum for FIB and conventional device is the larger thickness of TiW contact for the conventional device (approximately 150 \AA deviation from total 2000 \AA TiW film). This is prob-

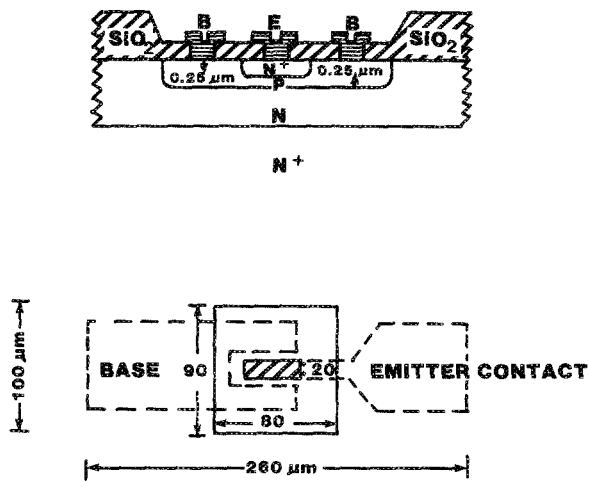


FIG. 1. Schematic of NPN bipolar transistor showing the emitter and base region.

ably due to process variation across the wafer. Additional RBS spectra were taken in the base and emitter regions and in surrounding regions near the base of FIB and conventional devices. No differences were detected in the RBS spectra for all devices, implying no microstructural differences between FIB and conventional implantation within the sensitivity of RBS.

In Fig. 3, we present the SAM spectra with the electron beam incident from the top of the device shown in Fig. 1. Figure 3(a) is the SAM spectra before sputtering through to the silicon and shows peaks indicating the presence of titanium and tungsten from the TiW contact barrier, nitrogen from the Si_3N_4 , and oxygen from the SiO_2 insulating layers. Figure 3(b) shows the spectrum at the same location just after sputter through to the Si. It can be seen that the Ti, W, N, and O peaks have all decreased in intensity. Finally, in Fig. 3(c) we show the SAM spectrum after sputter through to the

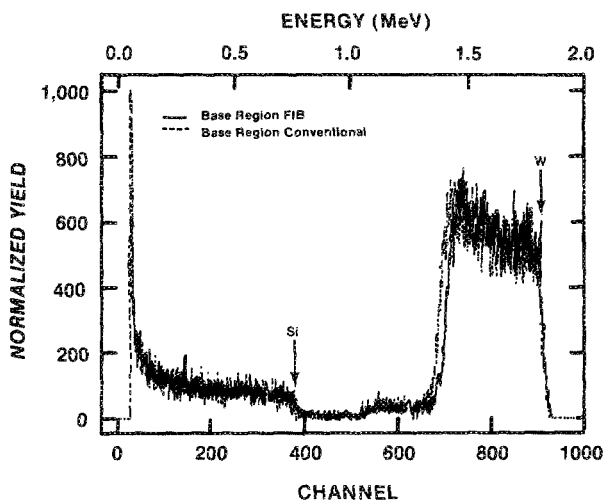
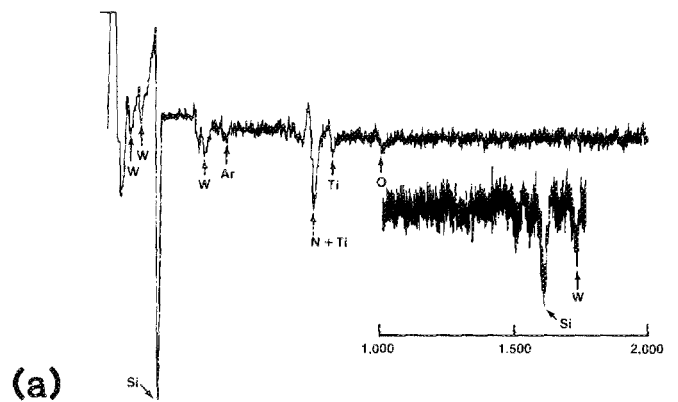
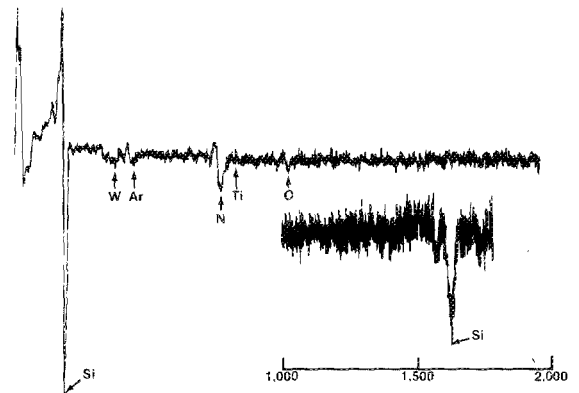


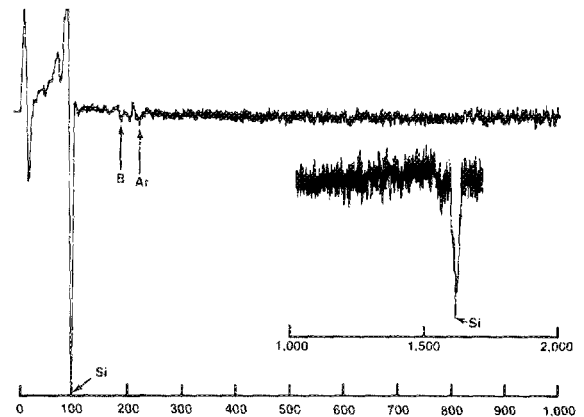
FIG. 2. RBS spectra for comparison of the base region of FIB and conventional devices.



(a)



(b)



(c)

FIG. 3. SAM spectra for the base region of FIB devices (a) before sputter through of Si, (b) sputter through to Si, (c) after sputter through of Si.

Si. Now the Ti, W, O, and N peaks have all disappeared. A slight hint of the presence of boron implanted in the base region can be seen in Fig. 3(c). Our main finding from the SAM measurements is that there are no unexpected impurities present in the devices.

B. Electrical characteristic analysis

A comparison of the general $I-V$ (I_{CE} vs V_{CE}) characteristics between FIB and conventional devices indicates no fundamental differences, even though the base doping profile of FIB transistors varies significantly. Table I shows all the

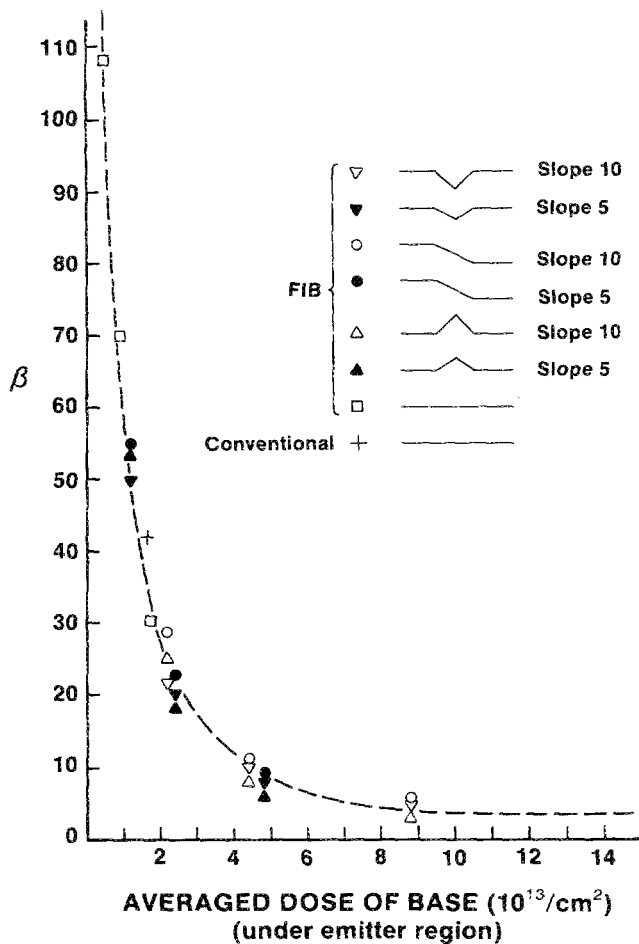


FIG. 4. Common emitter current gain vs the average dose of base under emitter region.

cases of the base doping profiles implanted and the device parameters measured. While the breakdown voltages change only slightly with doping, the correct trends (i.e., higher BV_{CEO} and lower BV_{CBO}) with increasing dose are observed. The similarity in electrical characteristics of the FIB and conventional implant devices provides an even more sensitive indication (compared to the RBS and SAM results) that there is no significant amount of either residual damage or contamination associated with FIB implanted boron.

The lateral profiles and doping densities reported in this study were intended to evaluate the feasibility of fabrication of transistors with lateral implant profiles, not provide optimum device performance. However, consideration of current gain (β) and base resistance (R_B) data as a function of doping and type of profile (Table I) highlights some interesting trends which will require more detailed study.

As shown in Fig. 4, the expected inverse relationship between β and average base dose under the emitter (base Gummel number, N_A) is observed. However, profile types 1 and 2 always have a 10%–20% lower β than the corresponding type 3–6 profiles for the same N_A (Table I). This is in qualitative agreement with expected results based on current crowding arguments. However, preliminary results⁹ indicat-

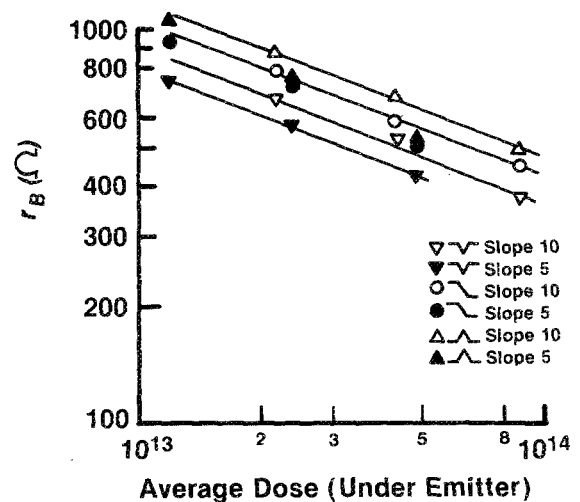


FIG. 5. Log-log plot for the base resistance vs average dose under the emitter region.

ed a greater variation in β with lateral profile. The discrepancy is thought to be due to the higher base implant dose (which lowers and minimizes differences in β) used in the present experiments.

Since R_B is a key parameter for transistors used in digital circuits, it is instructive to consider the effect of profile and doping for these devices. In Fig. 5 is plotted $\log R_B$ versus \log average dose under the emitter (active base). Clearly for the same intrinsic dose, R_B varies with profile due to the dose difference in the inactive (extrinsic) base. Types 1 and 2 (Table I) have heavy inactive base doping and low R_B . Types 5 and 6 (low inactive base doping) show the opposite behavior while Types 3 and 4 fall in between. These results are as expected. However, the trend observed in Fig. 5 suggests that a lateral profile with a fivefold change in dose (Type 2) has a lower R_B than a corresponding device with a tenfold change in active base doping (Type 1). The device data (Table I) provide specific examples of this observation if type 1A ($R_B = 655 \Omega$) versus 2B ($R_B = 575 \Omega$), and 1B ($R_B = 510 \Omega$) versus 2C ($R_B = 430 \Omega$) are compared. While some of the difference in R_B is due to a somewhat higher N_A for Type 2 profiles based on Fig. 5, a 10%–15% lower R_B would still be expected for equal total base doping density. Types 3 and 4 appear to show similar behavior, but for these profiles both the intrinsic and extrinsic doping densities are different, so only a qualitative observation is possible with the present data.

Taken together these results demonstrate the feasibility of fabricating bipolar transistors with lateral profiles in the active base. The device characteristics are consistent with expectations. More detailed experiments are required to determine the impact of profile type on β and R_B , but these results indicate that FIB can be used to fabricate the desired structures.

IV. CONCLUSIONS

The similarity of electrical properties, microstructures (RBS), and chemical constituents (SAM) indicate that to

within the sensitivity of the measurements there are no significant differences in focused and broad beam ion implantations in silicon interactions.

For the structures and dose used, a consistent relationship between the doping of the two regions of the base and the resulting electrical characteristics has been observed. While structures for optimum device performance have not yet been fabricated, the results demonstrate that lateral profiles do affect β and R_B . FIB therefore offers a means to examine the trade-off between β and R_B and studies of the impact of doping density and lateral profile type are proceeding.

ACKNOWLEDGMENTS

This research was supported in part by the Semiconductor Research Corporation. We thank Jeanne Denué and Karen Quirke for their assistance in preparation of the manuscript.

¹R. L. Kubena, C. L. Anderson, R. L. Seliger, R. A. Jullens, and E. H. Stevens, *J. Vac. Sci. Technol.* **19**, 916 (1984).

²E. Miyauchi, H. Arimoto, H. Hashimoto, and T. Utsumi, *J. Vac. Sci. Technol. B* **1**, 1113 (1983).

³T. Shiokawa, P. H. Kim, K. Toyada, and S. Namba, *J. Vac. Sci. Technol. B* **1**, 1117 (1983).

⁴R. L. Kubena, J. Y. M. Lee, R. A. Jullens, R. G. Bault, P. Middleton, and E. H. Stevens, *IEEE Trans. Electron Devices* **ED-31**, 1186 (1984).

⁵A. Wagner, D. L. Barr, T. Venkatesan, W. S. Crane, V. E. Lamberti, K. L. Tai, and R. G. Vadimsky, *J. Vac. Sci. Technol.* **19**, 1363 (1981).

⁶K. Gamo, Y. Ochiai, and S. Namba, *Jpn. J. Appl. Phys.* **21**, L792 (1982).

⁷H. Hamadeh, J. C. Corelli, A. J. Steckl, and I. L. Berry, *J. Vac. Sci. Technol. B* **3**, 91 (1985).

⁸I. L. Berry and A. L. Caviglia, *J. Vac. Sci. Technol. B* **1**, 1059 (1983).

⁹R. H. Reuss, D. Morgan, W. M. Clark, Jr., and D. B. Rensch, *J. Vac. Sci. Technol. B* **3**, 62 (1985).

¹⁰Y.-C. Liu, A. R. Neureuther, and W. G. Oldham, *J. Electrochem. Soc.* **130**, 939 (1983), and references therein.

¹¹V. Wang, J. W. Ward, and R. L. Seliger, *J. Vac. Sci. Technol.* **19**, 1158 (1981).

¹²W. G. Morris, W. Katz, H. Bakhr, and A. W. Haberl, *J. Vac. Sci. Technol. B* **3**, 391 (1985).

¹³Ian Getreu, *Modeling the Bipolar Transistor* (Tektronix, Beaverton, OR, 1976).